Electronic Supporting Information (ESI)

Characteristic growth of chemical gardens from mixtures of two salts

Yujin Kubodeda,[a] Yu Xu,[ab] Yuta Yamaguchi,[a] Muneyuki Matsuo,[a] Masashi Fujii,[a] Maya Kageyama,[c] Oliver Steinbock[d] and Satoshi Nakata*[a]

[a] Graduate School of Integrated Sciences for Life, Hiroshima University, 1-3-1 Kagamiyama, Higashi-Hiroshima 739-8526, Japan

[b] School of Chemistry and Chemical Engineering, Northwestern Polytechnical University, Chang'an campus 1 Dongxiang Road, Chang'an District, Xi'an Shaanxi, 710129, P. R. China

[c] School of Science, Kwansei Gakuin University, Sanda, Hyogo 669-1337, Japan

[d] Department of Chemistry and Biochemistry, Florida State University, Tallahassee, Florida 32306-4390, United States

*To whom correspondence should be addressed. Tel.: +81-824-24-7409

E-mail: nakatas@hiroshima-u.ac.jp

1. Movies S1-S4

Movie S1: The flow near the tip of the tube for $FeSO_4$ in Fig. 4a1 (side view, real time speed)
Movie S2: The flow near the tip of the tube for the mixture of $CaCl_2$ and $FeSO_4$ in Fig. 4a2 (side view, real time speed)
Movie S3: The flow near the tip of the tube for the mixture of $CuSO_4$ and $FeSO_4$ in Fig. 4a3 (side view, real time speed)
Movie S4: The flow near the tip of the tube for $CaCl_2$ (side view, real time speed)

2. Time-variation of the snapshots of chemical gardens for single metal salts

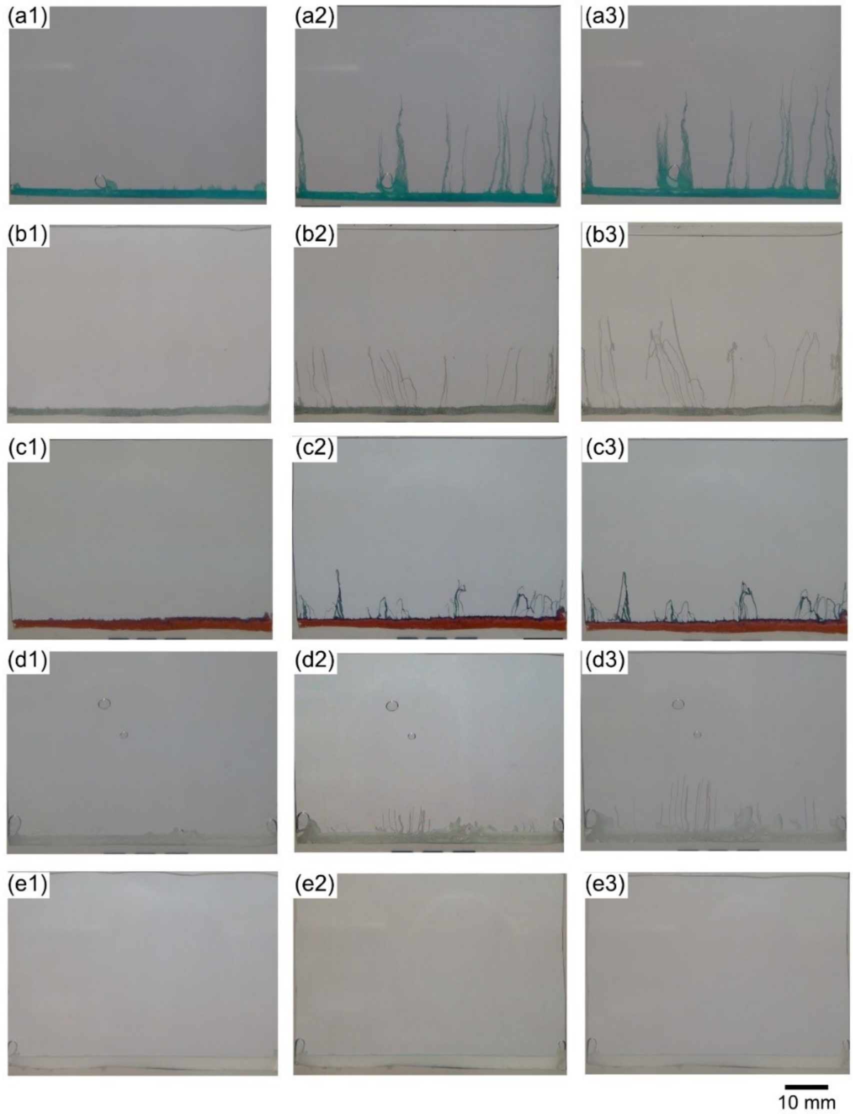

Fig. S1. Time variation of the snapshots for the single metal salts: (a) $CuSO_4$, (b) $FeSO_4$, (c) $CoSO_4$, (d) $CaCl_2$, and (e) $CaSO_4$. We recorded the photos at t = (1) 0, (2) 10, and (3) 20 min after the addition of the aqueous phase.

3. Time-variation of the average length of the tubes for single metal salts

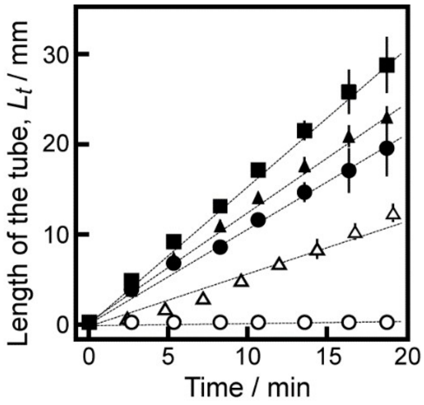

Fig. S2. Time-variation of the length of tubes, L_t, for single metal salts, $CuSO_4$ (filled rectangle), $FeSO_4$ (filled triangle), $CoSO_4$ (filled circle), $CaCl_2$ (empty triangle), and $CaSO_4$ (empty circle). The error bar represents the standard deviations as calculated from the three longest tubes. The data correspond to those in Fig. S1.

4. The effect the number density of the metal salt particles on the tube growth

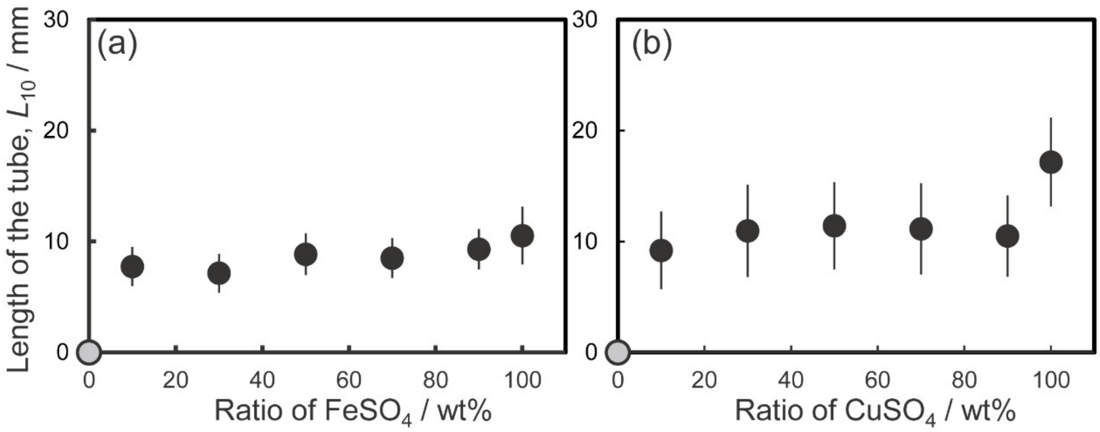

Fig. S3. Average values of L_{10} measured for different mixing ratios of the metal salt particles and glass beads: (a) $FeSO_4$ and (b) $CuSO_4$. The gray circle corresponds to the experimental condition of 100 wt% glass beads without metal salts. The error bars represent the standard deviations as calculated from the lengths of all tubes longer than 5 mm.

5. Snapshots of chemical gardens grown from mixtures composed of two different metal salts

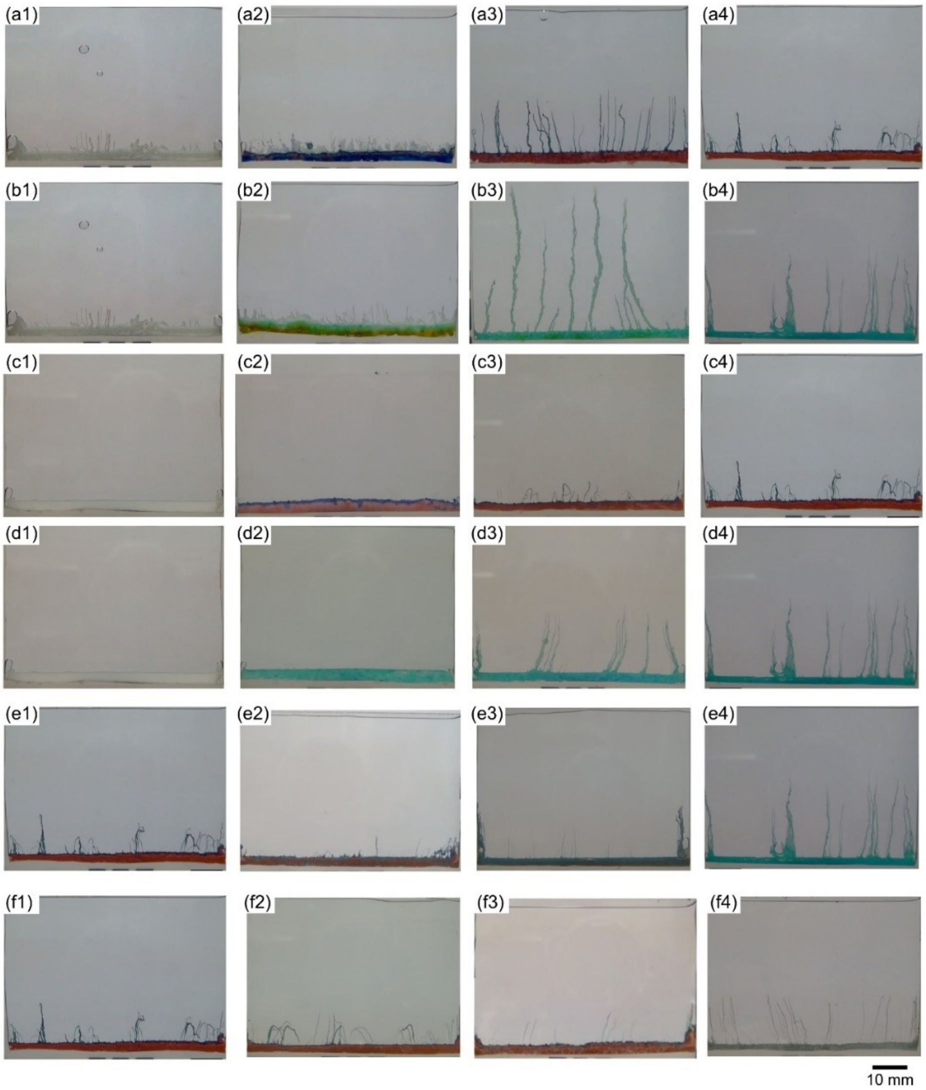

Fig. S4. Snapshots of chemical gardens from mixtures of A and B: (a) $CaCl_2$ and $CoSO_4$, (b) $CaCl_2$ and $CuSO_4$, (c) $CaSO_4$ and $CoSO_4$, (d) $CaSO_4$ and $CuSO_4$, (e) $CoSO_4$ and $CuSO_4$, and (f) $CoSO_4$ and $FeSO_4$. We recorded the photos at $t = 10$ min after the addition of the aqueous phase. The weight ratios of A and B, $W_A : W_B$ were (1) 100 : 0, (2) 70 : 30, (3) 30 : 70, and (4) 0 : 100.

6. Time-variation of the length of the tubes for mixtures composed of two different metal salts

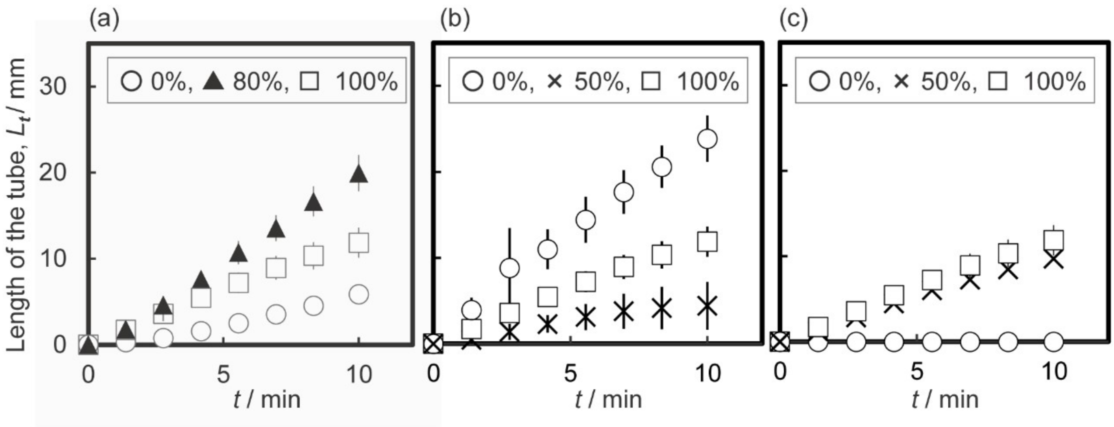

Fig. S5. Time-variation of the length of tubes, L_t, for the mixture of $FeSO_4$ with three different partner salts (PS): (a) $CaCl_2$, (b) $CuSO_4$, and (c) $CaSO_4$. The ratio of $FeSO_4$ is shown in the legend of each graph. The error bars represent the standard deviations as calculated from the three longest tubes. The data correspond to those in Fig. 3.

7. Length of the tube for the mixture of two kinds of metal salts

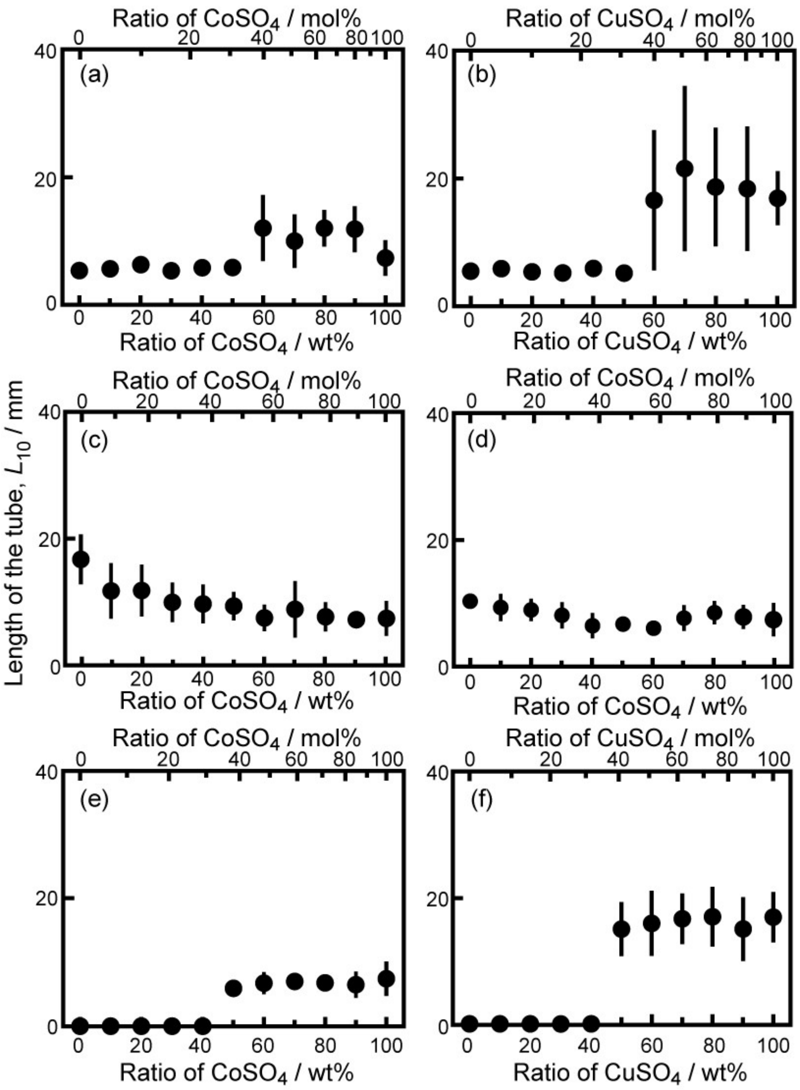

Fig. S6. Average values of L_{10} measured for different mixing ratios of A and B: (a) $CaCl_2$ and $CoSO_4$, (b) $CaCl_2$ and $CuSO_4$, (c) $CuSO_4$ and $CoSO_4$, (d) $FeSO_4$ and $CoSO_4$, (e) $CaSO_4$ and $CoSO_4$, and (f) $CaSO_4$ and $CuSO_4$. The upper and lower scale information refers to the molar ratio and the weight ratio, respectively. The error bars represent standard deviations as calculated from the lengths of all tubes longer than 5 mm.

8. Number and thickness of the tubes for mixtures of $FeSO_4$ with different partner salts

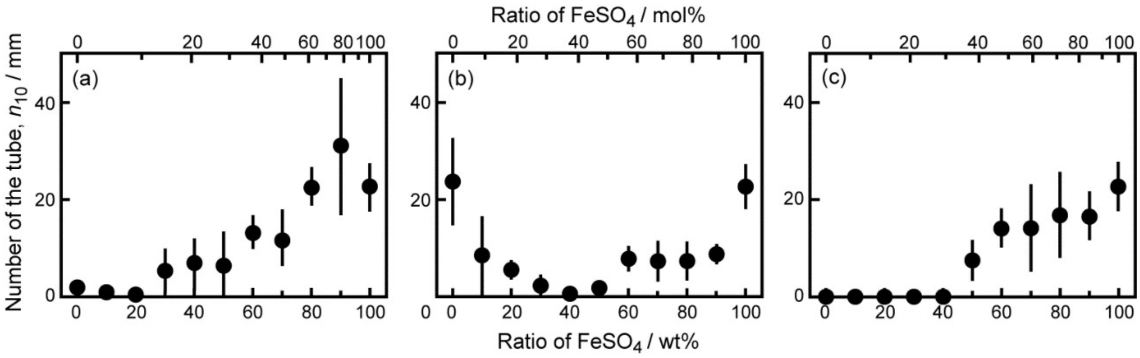

Fig. S7. Average values of n_{10} measured for different mixing ratios of $FeSO_4$ and one other metal salt: (a) $CaCl_2$, (b) $CuSO_4$, and (c) $CaSO_4$. The upper and lower scale information refers to the molar and the weight ratios, respectively. The error bars represent standard deviations as calculated from the number of tubes longer than 5 mm.

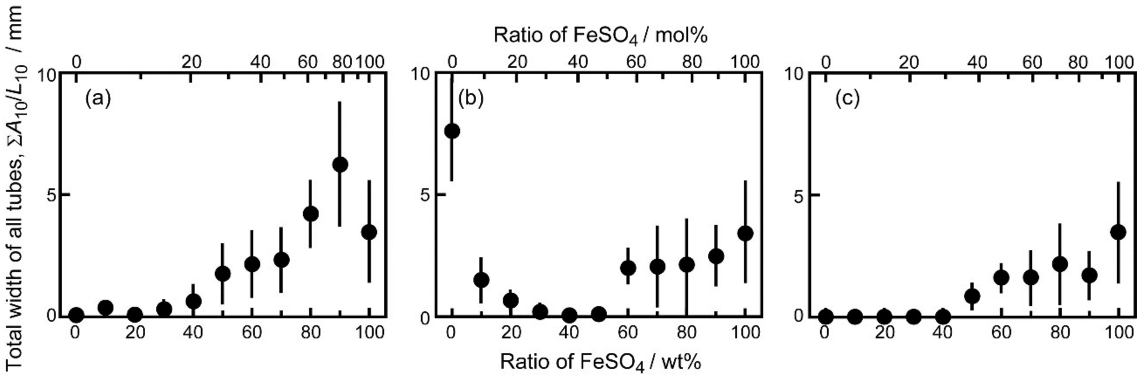

Fig. S8. Average values of $\Sigma A_{10}/L_{10}$ measured for different mixing ratios of $FeSO_4$ and one other metal salt: (a) $CaCl_2$, (b) $CuSO_4$, and (c) $CaSO_4$. The upper and lower scale information refers to the molar and the weight ratios, respectively. The error bars represent standard deviations.

9. Observation of the flow

We observed the flow rate near the tip of the tubes in our experimental setup. Actually, the same experimental procedure was followed except that 30 μL of spherical polymers (Fluoro-Max, model No. G0200, diameter: 2.0 μm) was added to 3 mL of 10 wt% Na_2SiO_3 aqueous solution, and the video camera was mounted on a microscope that was placed on its side. Fig. S9a shows time variation of the flow rate, F_t, for single $FeSO_4$, $CuSO_4$, $CaCl_2$ and the mixture of 20 wt% $CaCl_2$ and 80 wt% $FeSO_4$, and Fig. S9b shows that of 50 wt% $CuSO_4$ and 50 wt% $FeSO_4$.

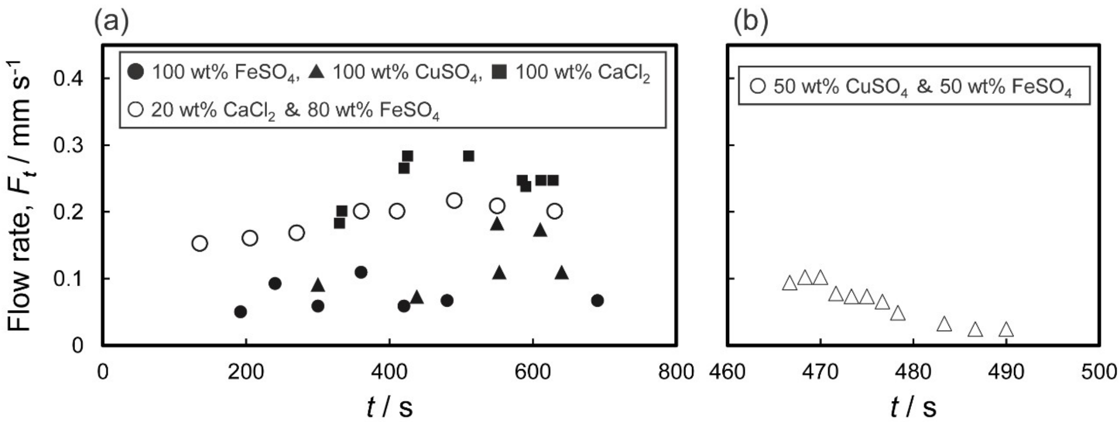

Fig. S9. Time variation of the flow rate, F_t for (a) 100 wt% $FeSO_4$, $CuSO_4$, $CaCl_2$ and the mixture of 20 wt% $CaCl_2$ and 80 wt% $FeSO_4$, and (b) 50 wt% $CuSO_4$ and 50 wt% $FeSO_4$.

10. Solubility, solubility product of metal salts, and the minimum concentration of metal ion to produce the precipitation

To consider the effect of the nature of metal salts, the solubility, solubility product of metal salts, and the minimum concentration of metal ion to produce the precipitation are shown in Table S1. Here, the minimum concentration of the metal ion is calculated by eqn (S1) based on the chemical reaction of reaction (2) in the main text.

$$[M^{2+}] = K_{sp}(M(OH)_2) / [OH^-]^2, \qquad (S1)$$

where $[M^{2+}]$ and $[OH^-]$ are the concentrations of a divalent cation and hydrogen oxide, respectively.

Table S1. The solubility in water of the metal salts and the solubility product of hydroxide product for the metal salts, K_{sp}, and the minimum concentration of metal ion.[1-3]

Metal salt	Solubility (mol / L water)	K_{sp} for $M(OH)_2$ (mol^3 / L^3)	Minimum conc. of metal ion (mol / L)
$CaSO_4 \cdot 2H_2O$	0.02	5.0×10^{-6}	5.0×10^{-2}
$CaCl_2$	6.71	5.0×10^{-6}	5.0×10^{-2}
$FeSO_4 \cdot 7H_2O$	1.06	8.0×10^{-16}	8.0×10^{-12}
$CoSO_4 \cdot 7H_2O$	2.14	1.6×10^{-15}	1.6×10^{-11}
$CuSO_4 \cdot 5H_2O$	0.92	2.2×10^{-20}	2.2×10^{-18}

11. Determination of the composition formula of silicate

According to the information of the reagent, silicate (Na_2O $nSiO_2$) is composed of 36.5 wt% SiO_2 and 18.0 wt% Na_2O. The molar ratio of SiO_2 and Na_2O, [SiO_2]/[Na_2O], is calculated as (36.5 wt% / 60.1 g mol^{-1})/(18.0 wt% / 62.0 g mol^{-1}) = 2.09. As $n = 2$, the formula of silicate may be described as $Na_2Si_2O_5$, as indicated in the reaction (2).

12. Dissolution rate of metal salts into the water phase

We measured the dissolution rate of metal salt in the water phase. Actually, 0.2 g of the metal salt powder was placed flat on the bottom of a glass cylinder (diameter: 13 mm, altitude of the powder: 4 mm), and 2 mL of water was slowly added onto the surface of metal salt powder. Actually, we measured the height of the solid phase and the dissolution rate was estimated based on the decreasing rate of height. We measured the dissolution rate by using eqn (S3) which was transformed from Noyes–Whitney equation (eqn S2).

$$\frac{dC}{dt} = k(C_{max} - C), \quad \text{(S2)}$$

$$kt = -ln(\frac{C_{max} - C}{C_{max}}), \quad \text{(S3)}$$

where k (s^{-1}) is rate constant of dissolution, t (s) is the time, C (M) is the dissolved concentration of the metal salt in the aqueous phase at time t, C_{max} (M) is the final value of C in Fig. S11a. Note that C was evaluated from the decrease in altitude of the solid phase. Fig. S11b shows the time variation of the value of kt (calculated by eqn (S3)). Table S2 shows the value of k which was fitted by the least-squares method from the line in Fig. S11b, and dissolution rate, dC/dt (M s^{-1}) when t = 0 calculated by eqn (S2).

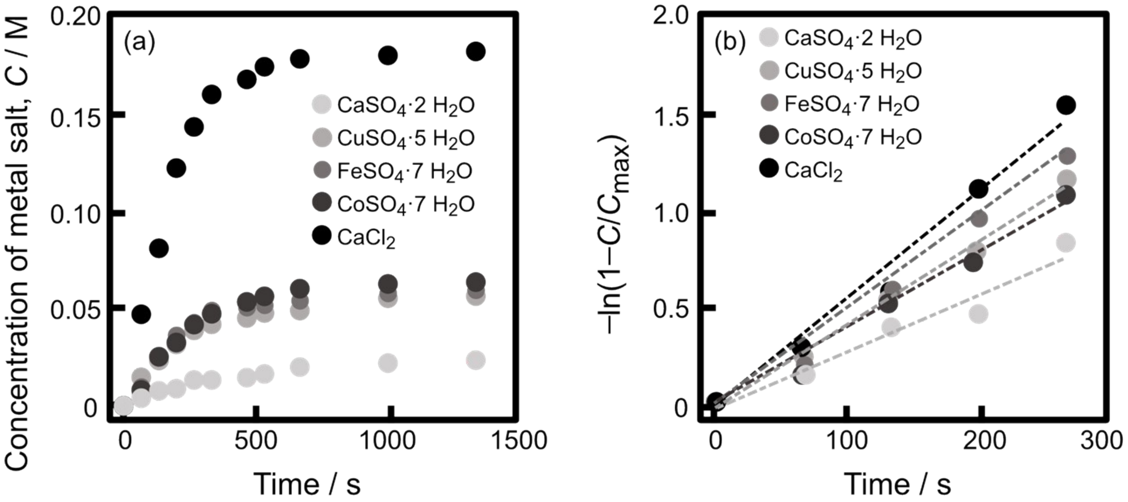

Fig. S10. Time variation of (a) C (M) and (b) kt calculated by eqn (S3).

Table S2. The rate constant of dissolution, k, and the dissolution rate of the metal salts in water.

Metal salt	Rate constant of dissolution, k / s^{-1}	Coefficient of determination for k	Dissolution rate at t = 0, $k\ C_{max}$ / M s^{-1}
$CaSO_4 \cdot 2H_2O$	2.7 x 10^{-3}	0.9885	0.64 x 10^{-4}
$CaCl_2$	5.2 x 10^{-3}	0.9831	9.5 x 10^{-4}
$FeSO_4 \cdot 7H_2O$	3.8 x 10^{-3}	0.9874	2.3 x 10^{-4}
$CoSO_4 \cdot 7H_2O$	4.2 x 10^{-3}	0.9978	2.7 x 10^{-4}
$CuSO_4 \cdot 5H_2O$	3.7 x 10^{-3}	0.9888	2.1 x 10^{-4}

References

S1. W. Zhao and K. Sakurai, *ACS Omega*, 2017, **2**, 4363–4369.

S2. J. H. E. Cartwright, B. Escribano and C. I. Sainz-Díaz, *Langmuir*, 2011, **27**, 3286–3293.

S3. Q. P. Wang, P. Knoll and O. Steinbock, *J. Phys. Chem. B*, 2021, **125**, 13908–13915.